IEEE Access
Multidisciplinary | Rapid Review | Open Access Journal

Received May 20, 2022, accepted May 27, 2022, date of publication June 2, 2022, date of current version June 9, 2022.

Digital Object Identifier 10.1109/ACCESS.2022.3179815

Fault-Tolerant Performance of the Novel Five-Phase Doubly-Fed Induction Generator

ROLAND RYNDZIONEK, (Senior Member, IEEE), KRZYSZTOF BLECHARZ, FILIP KUTT, MICHAL MICHNA, (Senior Member, IEEE), AND GRZEGORZ KOSTRO

Faculty of Electrical and Control Engineering, Gdansk University of Technology, 80-233 Gdansk, Poland

Corresponding author: Roland Ryndzionek (roland.ryndzionek@pg.edu.pl)

This work was supported by the Gdańsk University of Technology and IDUB Program under Grant 122020IDUBI.3.3.

ABSTRACT The article presents the concept of a new design of a multi-phase doubly-fed induction generator (DFIG). The innovative design approach uses a five-phase power supply from the rotor side of the generator with a three-phase classic stator power supply. Modern three-phase doubly-fed induction generators are the dominant choice for Wind Energy Conversion Systems (WECS). Solutions of this type are sensitive to the loss of at least one phase of the power supply from the rotor side due to the failure of the rotor side inverter. The proposed design solution in the form of a multi-phase power supply in the rotor circuit aims to extend the range of possible failure-free operation of the generator system, thus reducing system downtime due to the failure of power electronic systems. The correctness of the adopted conceptual assumptions was confirmed by the results of laboratory tests. The main contribution is to prove that using five-phase rotor winding improves the overall reliability of the proposed electrical energy generation system significantly.

INDEX TERMS Doubly-fed induction generator, induction generator, multi phase machine, wind power generation.

I. INTRODUCTION

The wind energy conversion technology began in the 1970s, but the real growth has been seen from the 1990s [1], [2]. These days, wind energy has become the most significant power generation capacity in Europe [3] with 220 GW of wind power capacity installed (195 GW onshore and 25 GW offshore). This rapidly growing wind energy market, especially in the last decade, requires the development of its key elements, e.g. generators, converters, and control algorithms.

Wind power generation systems, in the beginning, relayed on fixed or semi-fixed rotational velocity due to the usage of either synchronous generator (SG) or squirrel-cage induction generators (SCIG) that were connected to the grid directly [4], [5]. Generated power was controlled by the pitch of the wind turbine blades. However, the development of wind power generation technology led to the introduction of variable speed wind turbines, which in turn led to the development of the doubly-fed induction generator (DFIG) [5]–[9].

The associate editor coordinating the review of this manuscript and approving it for publication was R. K. Saket.

Nowadays, the topology based on the DFIG and permanent magnet synchronous generator (PMSG) is the most popular system and the widely used in modern wind power plants. The wind power generation system based on DFIG was developed in the late 19th century where two wound-rotor induction machines in cascade have been connected [10]. Since then, a variety of structures have been described, manufactured, and presented [11]–[15].

The principle of operation of such a system is based on an induction generator where stator and rotor winding is connected to the grid [16]–[19]. However, the rotor winding is connected to the grid by the converter and supplied via slip rings and back-to-back voltage or current source converters. The main advantage of such a system compared to PMSG is that only a portion of the generation system power needs to flow through the converter, improving the system's overall efficiency and allowing for the converter size to be significantly smaller than in SG or PMSG systems. [20], [21].

According to the advent of typologies based on back-to-back converters, multi-phase solutions have been under intensive investigation. However, most research concerns motor

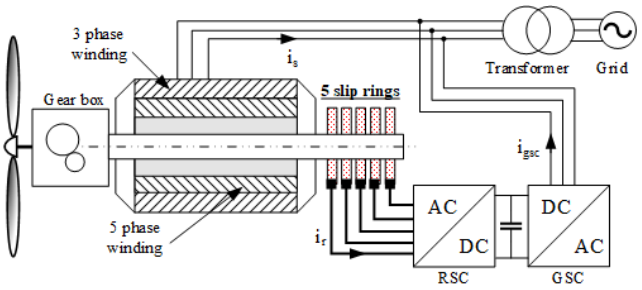

FIGURE 1. The scheme of the developed novel five-phase DFIG.

drives dedicated to electric vehicles or aircraft. In the literature, there are multi-phase (five, six, nine, and more stator winding) generators, but most of these solutions are dedicated to permanent magnets generators [22].

In general, the operation and control of multi-phase induction generators or motors under faulty conditions is an often-discussed problem now. In literature, there are many propositions of fault-tolerance strategy in terms of control in three-phase DFIG, e.g., current sensor fault-tolerant control [23], a fault-tolerant the instantaneous torque control (ITC) control strategy [24]. Moreover, the fault-tolerance in the multi-phase machine has been under investigation also. The [25] describes the study of the direct torque control method used in the normal operation of five-phase IM drives to the open-phase fault procedure. Moreover, [26] investigate optimal fault-tolerant control of multi-phase drives under open-phase faults. However, there is no study according multi-phase rotor winding in DFIG.

The authors developed the novel structure of the DFIG (Fig. 1). The key feature was to design the five-phase winding in the rotor structure and investigate its fault-tolerant capability compared to standard DFIG with 3 phase rotor winding. This kind of performance has not been investigated yet, and it is the main contribution of the presented study.

The paper is organized as follows: the structure of the developed five-phase DFIG and prototype validation FEA simulation is described in section II. The modeling and simulation of the prototype is presented in section III. In section IV, the prototype experimental analysis including fault tolerance operation is explained. Finally, the paper ends with a summary of the obtained results.

II. NOVEL 5-PHASE DFIG DEVELOPMENT

In modern electromechanical energy conversion systems, multi-phase machines are becoming more and more popular. However, until now, the major problem has been the control of such machines and the price of the dedicated power converter [27], [28]. Dynamic development of the semiconductors has resulted in wider availability of the various types of converters. Moreover, the prices of these converters have been reduced also. Thus, the large-scale application of multi-phase machines in the industry seems to be a matter of time [29].

The specifications of the prototype DFIGs used in this study are shown in Table 1. This generator has a six-pole,

TABLE 1. Main specifications of the studied five phase dfig.

Parameter	Machine	
Rated Power	Pn	4 kW
Voltage	Un	400V
Speed	nn	1000 rpm
Pair poles	p	3
Stator phases	ms	3
Rotor phases	mr	5
Stator slots	Qs	36
Stator turns in series per phase	Ns	203
Rotor slots	Qr	30
Rotor turns in series per phase	Nr	183
Rotor turns in series per coil	Nrs	61
Outer stator diameter	Dso	208
Inner stator diameter	Dsi	134
Airgap length	lg	0.3 mm
Axial length	ls	149 mm

three phases stator winding with one parallel branch and was constructed in the frame size of 132 mm. The generator has been developed using the original stator from a 5.5 kW Sg132m-6 induction motor.

The operating rotational velocity of the machine has been set as 700–1300 rpm and maximum power 5.3kW. This rotor range of operation affects the linear current density and nominal power of the designed rotor and would be the same for three and five phase DFIG considering the same current density and rotor volume. During the designing process, several key aspects have been considered - the current densities for the stator and rotor should not exceed 6 A/mm^2 and the maximum flux density of the teeth and the yokes in the stator and rotor are below 2.0 T.

The authors decide to use the original three-phase stator of the induction motor to be the stator of the developed generator. This stator was wounded to operate in delta (@ 400V) and star (@ 690V) configuration. However, because the machine is supposed to operate as a generator the stator was connected in star configuration at a nominal voltage of 400V. This approach leads to a decrease in the nominal power of the machine from 5.5 to 4 kW. Nevertheless, this allowed to decrease the flux density which in turn, allowed to increase the induced EMF for the generator operation and reduced the possibility of operation in high saturation conditions at higher than a nominal voltage level often present in power generation system nodes.

Proposed the research approach will allow for the generator uninterrupted power generation operation during converter or the rotor winding faulty operation. The fault-tolerant performance of the generation system will be achieved during single or dual rotor phase failure without a significant decrease in the machine stator power output.

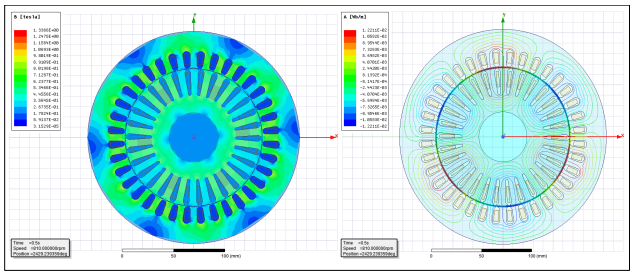

FIGURE 2. The FEA simulation of the flux density distribution in stator and rotor core.

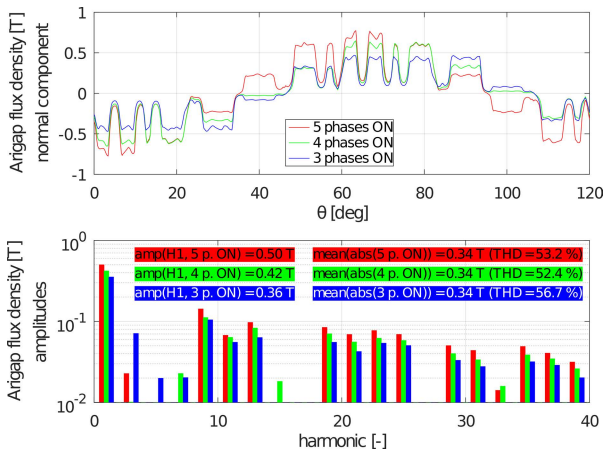

FIGURE 3. The airgap magnetic flux distribution. Red color is simulation with 5 rotor phase ON, blue and green colour is fault case with 4 rotor phase and 3 rotor phase ON respectively.

A. FEM ANALYSIS

The proposed DFIG design was verified using FEM simulations in Ansys Maxwell software. The full view 3D model of the five-phase DFIG has been designed using Autodesk Inventor and after that imported to the Anysys Maxwell.

The simulations were conducted to verify the analytical design calculated dimensions and parameters. Moreover, FEA was used to validate the designed prototype's capability in performing in different operating conditions.

Fig. 2 show the 2D FEM simulation of DFIG's flux density distribution, the maximum value of flux density is 1.4 T. The maximum value of flux density in airgap is 0.75 T (Fig. 3 red chart). The results fit in desired ranges. Moreover, the flux distribution corresponds to the stator and rotor slots distribution (no skewing is implemented in the 2D FEM model).

The fault-tolerant performance has been analyzed. The operation with one rotor phase failure has been simulated. The comparison is presented in Fig. 3. It could be noticed that, with 4 or 3 rotor phase ON, the average magnetic field is smaller than with 5 rotor phase ON. The distribution of the magnetic field is distorted but still has a sinusoidal shape. The difference in airgap flux distribution normal component THD is within 5 percentage point as show on Fig. 3.

The simulation results and laboratory measurements have been compared in chapter IV dedicated to prototype performance measurements.

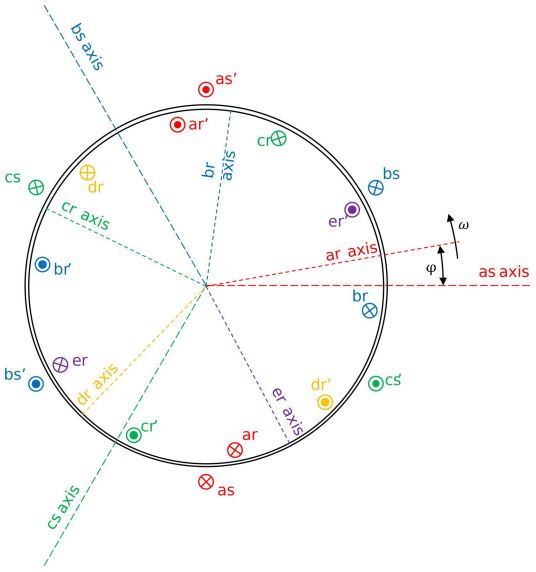

FIGURE 4. A simplified structure of the three phase stator and the five phase rotor DFIG.

III. MODELLING OF THE GENERATOR

The DFIG mathematical model was developed in a natural reference frame relaying stator parameters to the symmetric three-phase system of the stator and the rotor parameters to the symmetric five-phase system of the rotor. Such a model while relatively complex and requiring more computation power is more universal and enables simulations of the various generator operating states, e.g. loss of any excitation winding phase.

Fig. 4 shows a simplified structure of the newly developed DFIG consisting of three stator phases and five rotor phases. The stator windings are marked with the letter s and the rotor winding with the letter r.

General structure of the five-phase DFIG model is based on the voltage and linkage flux equations of the stator and rotor windings [30]. The stator and rotor voltage equations are defined as:

$$\begin{bmatrix} V_s \\ V_r \end{bmatrix} = \begin{bmatrix} R_s & 0 \\ 0 & R_r \end{bmatrix} \begin{bmatrix} I_s \\ I_r \end{bmatrix} + \frac{\mathrm{d}}{\mathrm{d}t} \begin{bmatrix} \Psi_s \\ \Psi_r \end{bmatrix}, \tag{1}$$

where: V_s, V_r- stator and rotor voltage vectors,I_s, I_r- stator and rotor current vectors, R_s, R_r- stator and rotor diagonal resistance matrices, Ψ_s, Ψ_r- stator and rotor flux linkage vectors.

The voltage, current and flux linkage vectors of the stator and rotor windings are defined as:

$$(f_s)^{\mathrm{T}} = \begin{bmatrix} f_{as} & f_{bs} & f_{cs} \end{bmatrix}, \tag{2}$$

$$(f_r)^{\mathrm{T}} = \begin{bmatrix} f_{ar} & f_{br} & f_{cr} & f_{dr} & f_{er} \end{bmatrix}. \tag{3}$$

The flux linkage equation for the stator and rotor winding are defined as:

$$\begin{bmatrix} \Psi_s \\ \Psi_r \end{bmatrix} = \begin{bmatrix} L_{ss} & L_{sr}(\varphi) \\ L_{rs}(\varphi) & L_{rr} \end{bmatrix} \begin{bmatrix} I_s \\ I_r \end{bmatrix}, \tag{4}$$

where: L_{ss} - inductance matrix of stator winding, L_{rr} - inductance matrix of rotor winding, $L_{sr} = L_{rs}^{\mathrm{T}}$- – the matrix

TABLE 2. Electrical Parameters Of The Studied Five Phase DFIG.

Parameter	Machine	
Stator resistance	Rs	2.5 ohm
Rotor resistance	Rr	2.27 ohm
Stator magnetizing inductance	Lms	334 mH
Stator leakage inductance	Lls	45 mH
Rotor magnetizing inductance	Lmr	252 mH
Rotor leakage inductance	Llr	34 mH
Mutual inductance	Lsr	290 mH

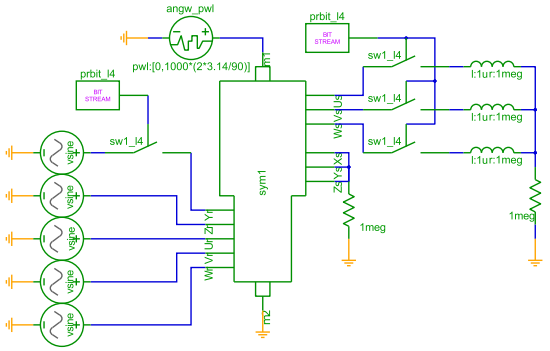

FIGURE 5. Synopsys Saber simulation wiring diagram.

of mutual inductances between stator and rotor windings, φ - rotor angle.

The DFIG model (1) completes the mechanical equation:

$$t_{em} = t_l + J\frac{\mathrm{d}\omega}{\mathrm{d}t} + D\omega, \tag{5}$$

where: t_{em} - electromagnetic torque, t_l - load torque, J - moment of inertia, $\omega = \frac{\mathrm{d}\varphi}{\mathrm{d}t}$ - rotor angular velocity, D - the mechanical damping constant.

The electromagnetic torque is determined from the equation:

$$t_{em} = \frac{1}{2}\left[I_s^{\mathrm{T}}\ I_r^{\mathrm{T}}\right]\frac{\partial}{\partial\varphi}\begin{bmatrix} L_{ss} & L_{sr}(\varphi) \\ L_{rs}(\varphi) & L_{rr}\end{bmatrix}\begin{bmatrix} I_s \\ I_r\end{bmatrix}. \tag{6}$$

Detailed forms of the variables appearing in equations (1), (4) and (6) are listed in the appendix. The electric parameters have been determined based on design specification and measurements (Table 2).

Using similar approach a model of standard three phase DFIG was also developed. Both models were than implemented in Synopsys Saber simulator using MAST language. The purpose of this effort was to compare and investigate the behavior under the rotor phase failure in case of 3 and 5 phase rotor DFIG.

The simulations for both the standard 3 phases rotor and novel 5 phase rotor DFIG were conducted under similar conditions:

- both machines operating in no-load, off-grid conditions,
- before the failure, the rotor winding of both machines are supplied with voltage sources allowing for the rotor current to produce nominal stator voltage,

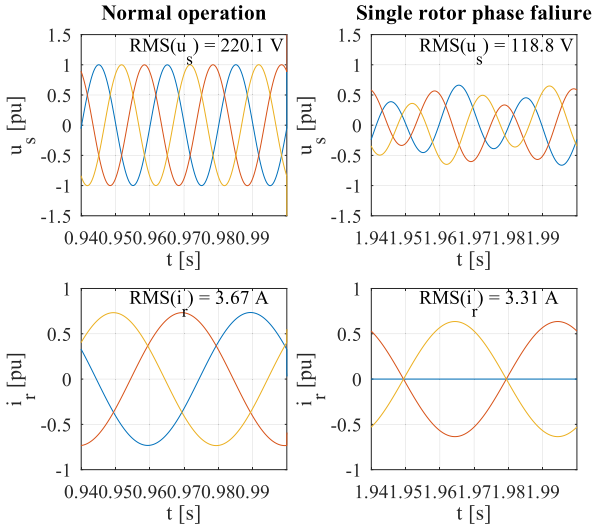

FIGURE 6. Standard 3 phase rotor DFIG normal and with single phase failure, off grid, no load performance stator voltage (u_s) and rotor current(i_r) waveforms.

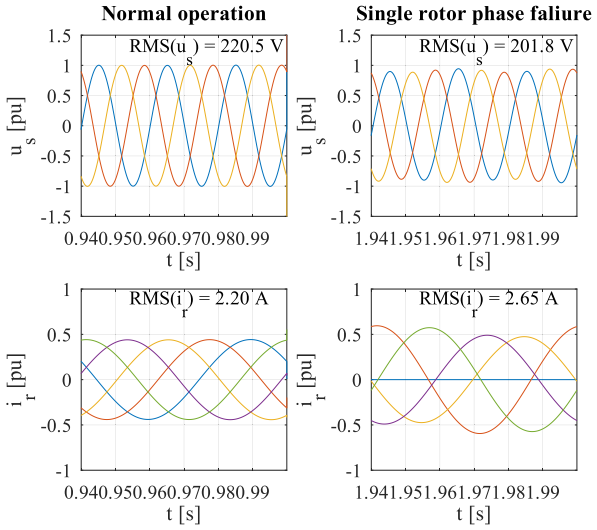

FIGURE 7. Novel 5 phase rotor DFIG normal and with single phase failure, off grid, no load performance stator voltage (u_s) and rotor current(i_r) waveforms.

- both machines operate with the rotor supply voltage frequency of 13.5 Hz and rotor rotational velocity of 730 rpm, producing stator voltage with a frequency of 50 Hz,
- during the failure test in both cases single rotor phase voltage source is disconnected.

Firstly, the simulation results for 3 phase rotor DFIG, off-grid, no-load performance have been performed. The results are presented in Fig. 6. We can observe that single rotor phase failure impacts the stator voltage significantly, the amplitude is around 50% of nominal voltage.

In the case of novel 5 phases machine the results are shown in Fig. 7. It can be observed that single phase failure has a much lower impact on the machine stator voltage compared to 3 phase rotor machine, the voltage amplitude is around 90%

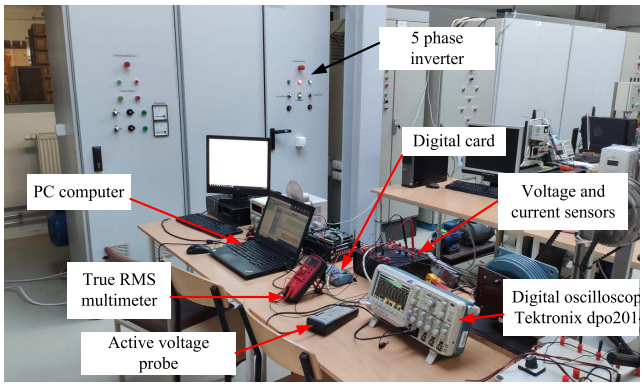

FIGURE 8. a) The laboratory test bench of the five-phase DFIG prototype.

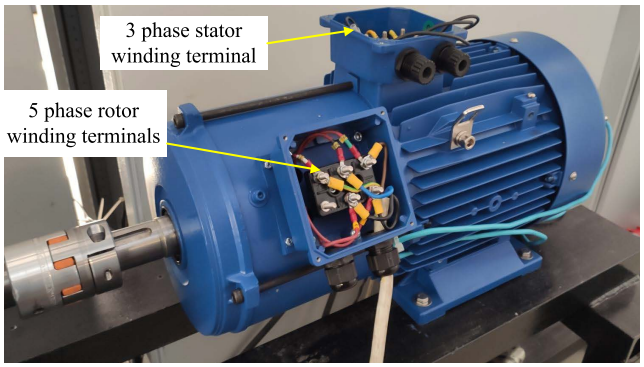

FIGURE 9. The laboratory prototype five-phase DFIG.

of nominal voltage compared to 50% in case of 3 phase rotor machine. This behaviour is understandable, however, what is more important rotor excitation current in five phase DFIG increases during the failure test and in 3 phase machine it decreased. This also is something to be expected, however it shows natural capability of 5 phase rotor machine to accommodate for rotor phase failure.

The use of five phase winding shows a huge advantage over three phase standard system. The current in rotor winding has small amplitude fluctuations, and the phase angle has changed as well. It should be noticed that these simulation results have been made without any control algorithms. The application of the control algorithms should improve generator performance further.

IV. LABORATORY TESTS

In this paper, measurements are carried out to analyze and validate the performances benefits of the proposed five-phase DFIG and to verify the developed prototype construction (Fig. 8).

The main purpose of the laboratory tests was to verify the fault tolerance of the novel five-phases DFIG. In the laboratory test bench, the five-phase DFIG (Fig. 9) is driven by the 5.5 kW induction motor. The mechanical speed of the motor is adjusted by an inverter control unit. The 5.5 KW induction motor is mechanically coupled with a five-phase DFIG. This configuration of the drive system enables regulation of the generator rotational speed in a wide range.

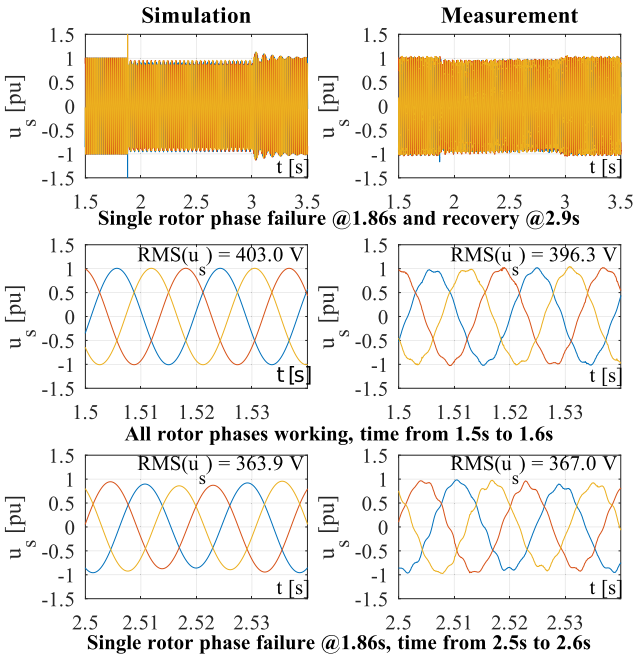

FIGURE 10. The laboratory test of one rotor phase failure - no-load test. The voltage waveform with one phase OFF.

The prototype generator measurements were carried out in an open-loop off-grid power generation system. The five-phase rotor winding was supplied from a five-phase voltage inverter, while the stator winding was connected to a variable three-phase load. This connection corresponds to the configuration of the generator operating in the stand-alone mode. The voltage inverter allowed for smooth adjustment of the five-phase rotor voltage amplitude and frequency. The two-level voltage inverter is a structure entirely developed at the Gdansk University of Technology. The control system of the converter was implemented on a microprocessor system with a floating-point digital signal processor (ADSP21363) with a sampling time of 150 us and a field-programmable gate array device (Intel/Altera Cyclone II). The inverter operates with a transistor switching frequency twice of the control sampling time, i.e., 3.3 kHz.

The research results presented in the paper were acquired without the use of a closed-loop control system in the control structure of the inverter. In such a scenario, the inverter supplying the rotor circuit can be treated as a non-inertial controlled voltage and frequency source with a high precision of reference parameters set by the user.

A. FAULT TOLERANT PERFORMANCE

The fault-tolerant performance of the proposed novel five-phase DFIG was analyzed. First of all, the no-load test has been performed. After that, the tests with different electric load levels were conducted. The single and dual-phase failures have been applied to the rotor of the generation system during the operation. The performed measurements are conducted during the disconnection of rotor phases A and/or C.

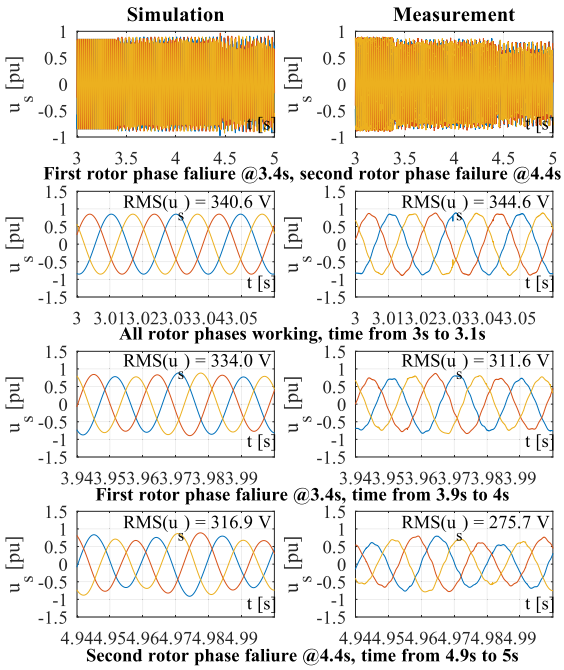

FIGURE 11. The reliability laboratory test of rotor phases failure. Stator voltage waveforms. The generator is under active resistive load.

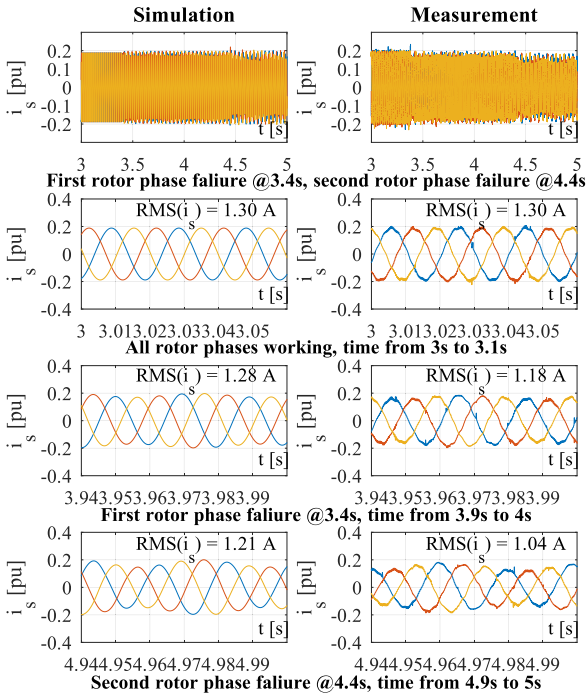

FIGURE 12. The reliability laboratory test of rotor phases failure. Stator current waveforms. The generator is under active resistive load.

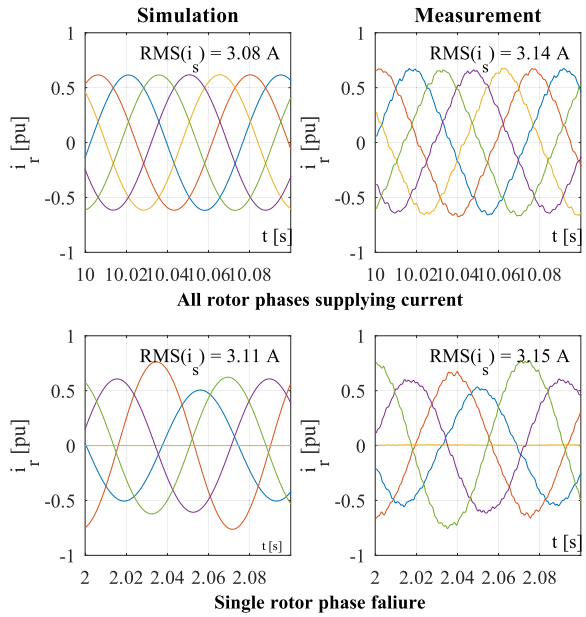

FIGURE 13. The reliability laboratory test of rotor phases failure. Rotor current waveforms in different fault phase case. The generator is under active resistive load.

In Fig. 10 the rotor phase A is briefly disconnected during the machine operation in no-load conditions (Pashe A - ON, Phase A - OFF, Phase A - ON). As could be noticed, the stator voltage drops approx. 30V. Despite the one rotor phase being disconnected the stator voltage waveform shape is not affected, however, small asymmetry in the stator three-phase system could be noticed. The measured stator RMS voltages on each phase differ by about $5 \div 8$ V.

In the load conditions (Fig. 11) a single rotor phase failure also causes the decrease in amplitude and the asymmetry in stator voltage and the dual rotor failure exacerbates this even further. However, because the voltage is still generated this indicates that the excitation five-phase converter algorithm can be developed to mitigate the changes in amplitude and shape of the airgap flux distribution for adequate fault-tolerant performance. Moreover, the same tendency could be noticed in stator currents (Fig. 12). The asymmetry appears under the rotor failure however the stator current is still sinusoidal. The active power in single and dual rotor failure decreased by 20% and 50% respectively.

Fig. 13 presents the current waveforms in different phase fault cycles. The laboratory test is consistent with the simulation results. It can be seen that the amplitude of the individual phases and the phase angles change. The five phase DFIG behaves exactly as the simulation showed.

In general, the obtained reliability tests are far more than acceptable to state that the proposed approach allows for the generation system fault-tolerant performance concerning the rotor winding single or dual phase failure. It should be emphasized that the measurements were conduct in open-loop without any control algorithms. This will be the next study in the authors research series.

V. CONCLUSION

In summary, this paper proposes a novel five-phase DFIG to introduce a fault-tolerant generation system dedicated to modern wind power plants. The proposed generator has been developed and a prototype machine has been manufactured and tested under different operating conditions. The paper presents the complete research cycle with analytical modeling, FEA simulations, and laboratory tests. From both the

simulations and measurements, obtained results have been compared and commented on.

It should be noted that the tests carried out were performed for non-nominal operating conditions - under-nominal voltage and under the rotational velocity within the nominal range. However, the presented five-phase DFIG shows adequate performance during laboratory tests in all investigated operation conditions. The five-phase DFIG has a significant advantage over existing constructions, an operation with a damaged excitation phase (or even two phases). It is possible to use six or more phases in the rotor winding. However, the 5-phase winding, after the 3-phase winding, offers the possibility of generating a rotating magnetic field. Currently, the authors are working on a closed-loop control system for fault-tolerant on-grid performance.

APPENDIX

Stator and rotor voltage vectors:

$$\begin{aligned}(V_s)^{\mathrm{T}} &= \left[v_{as}\ v_{bs}\ v_{cs}\right],\\ (V_r)^{\mathrm{T}} &= \left[v_{ar}\ v_{br}\ v_{cr}\ v_{dr}\ v_{er}\right].\end{aligned} \tag{7}$$

Stator and rotor current vectors:

$$\begin{aligned}(I_s)^{\mathrm{T}} &= \left[i_{as}\ i_{bs}\ i_{cs}\right],\\ (I_r)^{\mathrm{T}} &= \left[i_{ar}\ i_{br}\ i_{cr}\ i_{dr}\ i_{er}\right].\end{aligned} \tag{8}$$

Stator and rotor flux linkage vectors:

$$\begin{aligned}(\Psi_s)^{\mathrm{T}} &= \left[\psi_{as}\ \psi_{bs}\ \psi_{cs}\right],\\ (\Psi_r)^{\mathrm{T}} &= \left[\psi_{ar}\ \psi_{br}\ \psi_{cr}\ \psi_{dr}\ \psi_{er}\right].\end{aligned} \tag{9}$$

The diagonal stator and rotor resistance matrices are defined as:

$$R_s = diag(R_{as}, R_{bs}, R_{cs}),$$

$$R_r = diag(R_{ar}, R_{br}, R_{cr}, R_{dr}, R_{er}). \tag{10}$$

The inductance matrix for three phase symmetrical stator windings system is defined by:

$$L_{ss} = \begin{bmatrix} L_{ls}+L_{ms} & -\frac{1}{2}L_{ms} & -\frac{1}{2}L_{ms} \\ -\frac{1}{2}L_{ms} & L_{ls}+L_{ms} & -\frac{1}{2}L_{ms} \\ -\frac{1}{2}L_{ms} & -\frac{1}{2}L_{ms} & L_{ls}+L_{ms} \end{bmatrix}, \tag{11}$$

where stator self-inductance are the sum of a leakage inductance (L_{ls}) and a magnetizing inductance (L_{ms}).

The inductance matrix of five-phase symmetrical rotor winding is as (12), shown at the bottom of the page, where L_{lr} is a rotor leakage inductance and L_{mr} is a rotor magnetizing inductance.

The mutual inductances matrix between three phase stator and five-phase rotor winding is defined as (13), shown at the bottom of the page, where p is the number of pole pairs and Lsr is maximal mutual inductance between stator and rotor winding.

The electromagnetic torque is given by:

$$\begin{aligned} t_{em} = -pL_{sr}\Big\{ & i_{ar}\Big[\sin(p\varphi)\, i_{as} \\ & + \sin(p\varphi - 2/3\,\pi)\, i_{bs} \\ & + \sin(p\varphi + 2/3\,\pi)\, i_{cs}\Big] \\ & + i_{br}\Big[\sin(p\varphi + 2/5\,\pi)\, i_{as} \\ & + \sin(p\varphi + 2/5\,\pi - 2/3\,\pi)\, i_{bs} \\ & + \sin(p\varphi + 2/5\,\pi + 2/3\,\pi)\, i_{cs}\Big] \\ & + i_{cr}\Big[\sin(p\varphi + 4/5\,\pi)\, i_{as} \\ & + \sin(p\varphi + 4/5\,\pi - 2/3\,\pi)\, i_{bs} \end{aligned}$$

$$L_{rr} = L_{lr}\begin{bmatrix} 1 & & & & \\ & 1 & & & \\ & & 1 & & \\ & & & 1 & \\ & & & & 1 \end{bmatrix} + L_{mr}\begin{bmatrix} 1 & \cos\left(\frac{2}{5}\pi\right) & \cos\left(\frac{4}{5}\pi\right) & \cos\left(\frac{4}{5}\pi\right) & \cos\left(\frac{2}{5}\pi\right) \\ \cos\left(\frac{2}{5}\pi\right) & 1 & \cos\left(\frac{2}{5}\pi\right) & \cos\left(\frac{4}{5}\pi\right) & \cos\left(\frac{4}{5}\pi\right) \\ \cos\left(\frac{4}{5}\pi\right) & \cos\left(\frac{2}{5}\pi\right) & 1 & \cos\left(\frac{2}{5}\pi\right) & \cos\left(\frac{4}{5}\pi\right) \\ \cos\left(\frac{4}{5}\pi\right) & \cos\left(\frac{4}{5}\pi\right) & \cos\left(\frac{2}{5}\pi\right) & 1 & \cos\left(\frac{2}{5}\pi\right) \\ \cos\left(\frac{2}{5}\pi\right) & \cos\left(\frac{4}{5}\pi\right) & \cos\left(\frac{4}{5}\pi\right) & \cos\left(\frac{2}{5}\pi\right) & 1 \end{bmatrix}, \tag{12}$$

$$L_{rs(\varphi)} = \left(L_{sr(\varphi)}\right)^{\mathrm{T}} = L_{sr}\begin{bmatrix} \cos(p\varphi) & \cos\left(p\varphi - \frac{2}{3}\pi\right) & \cos\left(p\varphi + \frac{2}{3}\pi\right) \\ \cos\left(p\varphi + \frac{2}{5}\pi\right) & \cos\left(p\varphi - \frac{4}{15}\pi\right) & \cos\left(p\varphi - \frac{14}{15}\pi\right) \\ \cos\left(p\varphi + \frac{4}{5}\pi\right) & \cos\left(p\varphi + \frac{2}{15}\pi\right) & \cos\left(p\varphi - \frac{8}{15}\pi\right) \\ \cos\left(p\varphi + \frac{6}{5}\pi\right) & \cos\left(p\varphi + \frac{8}{15}\pi\right) & \cos\left(p\varphi - \frac{2}{15}\pi\right) \\ \cos\left(p\varphi + \frac{8}{5}\pi\right) & \cos\left(p\varphi + \frac{14}{15}\pi\right) & \cos\left(p\varphi + \frac{4}{15}\pi\right) \end{bmatrix}, \tag{13}$$

$$+\sin(p\varphi + 4/5\,\pi + 2/3\,\pi)\,i_{cs}\Big]$$
$$+i_{dr}\Big[\sin(p\varphi - 4/5\,\pi)\,i_{as} + \sin(p\varphi - 4/5\,\pi - 2/3\,\pi)\,i_{bs} + \sin(p\varphi - 4/5\,\pi + 2/3\,\pi)\,i_{cs}\Big]$$
$$+i_{er}\Big[\sin(p\varphi - 2/5\,\pi)\,i_{as} + \sin(p\varphi - 2/5\,\pi - 2/3\,\pi)\,i_{bs} + \sin(p\varphi - 2/5\,\pi + 2/3\,\pi)\,i_{cs}\Big]\Big\}. \quad (14)$$

ACKNOWLEDGMENT

The authors would like to thank the MESCO, an authorized distributor of ANSYS, for granting the Ansys Electronics Desktop license.

REFERENCES

[1] M. Cheng and Y. Zhu, "The state of the art of wind energy conversion systems and technologies: A review," *Energy Convers. Manage.*, vol. 88, pp. 332–347, Dec. 2014.
[2] S. Müller, M. Deicke, and R. W. D. Doncker, "Doubly fed induction generator systems for wind turbines," *IEEE Ind. Appl. Mag.*, vol. 8, no. 3, pp. 26–33, May/Jun. 2002.
[3] I. Komusanac, G. Brindley, D. Fraile, and L. Ramirez, "Wind energy in Europe 2020 statistics and the outlook for 2021–2025," Wind Eur. Bus. Intell., Brussels, Belgium, Tech. Rep., 2021.
[4] F. Kutt, M. Michna, and G. Kostro, "Multiple reference frame theory in the synchronous generator model considering harmonic distortions caused by nonuniform pole shoe saturation," *IEEE Trans. Energy Convers.*, vol. 35, no. 1, pp. 166–173, Mar. 2020. [Online]. Available: https://ieeexplore.ieee.org/document/8892641/
[5] Y. Song and F. Blaabjerg, "Overview of DFIG-based wind power system resonances under weak networks," *IEEE Trans. Power Electron.*, vol. 32, no. 6, pp. 4370–4394, Jun. 2017.
[6] E. L. Soares, C. B. Jacobina, V. F. M. B. Melo, N. Rocha, and E. R. C. da Silva, "Dual converter connecting open-end doubly fed induction generator to a DC-microgrid," *IEEE Trans. Ind. Appl.*, vol. 57, no. 5, pp. 5001–5012, Sep. 2021.
[7] S. Baros and M. D. Ilic, "Distributed torque control of deloaded wind DFIGs for wind farm power output regulation," *IEEE Trans. Power Syst.*, vol. 32, no. 6, pp. 4590–4599, Nov. 2017.
[8] F. Blaabjerg, M. Liserre, and K. Ma, "Power electronics converters for wind turbine systems," *IEEE Trans. Ind. Appl.*, vol. 48, no. 2, pp. 708–719, Mar./Apr. 2012.
[9] G. D. Marques and M. F. Iacchetti, "DFIG topologies for DC networks: A review on control and design features," *IEEE Trans. Power Electron.*, vol. 34, no. 2, pp. 1299–1316, Feb. 2019. [Online]. Available: https://ieeexplore.ieee.org/document/8345779/
[10] T. D. Strous, H. Polinder, and J. A. Ferreira, "Brushless doubly-fed induction machines for wind turbines: Developments and research challenges," *IET Elect. Power Appl.*, vol. 11, no. 6, pp. 991–1000, Jul. 2017.
[11] P. Han, M. Cheng, X. Wei, and Y. Jiang, "Steady-state characteristics of the dual-stator brushless doubly fed induction generator," *IEEE Trans. Ind. Electron.*, vol. 65, no. 1, pp. 200–210, Jan. 2018.
[12] M. Adamowicz and R. Strzelecki, "Cascaded doubly fed induction generator with a back-to-back converter connected to a small distributed generation system," 2009.
[13] A. Čeponis, D. Mažeika, and P. Vasiljev, "Flat cross-shaped piezoelectric rotary motor," *Appl. Sci.*, vol. 10, no. 14, p. 5022, Jul. 2020. [Online]. Available: https://www.mdpi.com/2076-3417/10/14/5022
[14] A. Beainy, C. Maatouk, N. Moubayed, and F. Kaddah, "Comparison of different types of generator for wind energy conversion system topologies," in *Proc. 3rd Int. Conf. Renew. Energies Developing Countries (REDEC)*, Jul. 2016, pp. 1–6.
[15] X. Wei, M. Cheng, J. Zhu, H. Yang, and R. Luo, "Finite-set model predictive power control of brushless doubly fed twin stator induction generator," *IEEE Trans. Power Electron.*, vol. 34, no. 3, pp. 2300–2311, Mar. 2019. [Online]. Available: https://ieeexplore.ieee.org/document/8374973/
[16] H. Misra and A. K. Jain, "Analysis of stand-alone DFIG-DC system and DC voltage regulation with reduced sensors," *IEEE Trans. Ind. Electron.*, vol. 64, no. 6, pp. 4402–4412, Jun. 2017.
[17] D. Ochoa and S. Martinez, "Fast-frequency response provided by DFIG-wind turbines and its impact on the grid," *IEEE Trans. Power Syst.*, vol. 32, no. 5, pp. 4002–4011, Sep. 2017.
[18] D. Wachowiak, "A universal gains selection method for speed observers of induction machine," *Energies*, vol. 14, no. 20, p. 6790, Oct. 2021. [Online]. Available: https://www.mdpi.com/1996-1073/14/20/6790
[19] L. Huang, H. Xin, L. Zhang, Z. Wang, K. Wu, and H. Wang, "Synchronization and frequency regulation of DFIG-based wind turbine generators with synchronized control," *IEEE Trans. Energy Convers.*, vol. 32, no. 3, pp. 1251–1262, Sep. 2017.
[20] D. Zhou, G. Zhang, and F. Blaabjerg, "Optimal selection of power converter in DFIG wind turbine with enhanced system-level reliability," *IEEE Trans. Ind. Appl.*, vol. 54, no. 4, pp. 3637–3644, Jul./Aug. 2018.
[21] Y. Song, X. Wang, and F. Blaabjerg, "Doubly fed induction generator system resonance active damping through stator virtual impedance," *IEEE Trans. Ind. Electron.*, vol. 64, no. 1, pp. 125–137, Jan. 2017. [Online]. Available: http://ieeexplore.ieee.org/document/7539594/
[22] Y. Chen and B. Liu, "Design and analysis of a five-phase fault-tolerant permanent magnet synchronous motor for aerospace starter-generator system," *IEEE Access*, vol. 7, pp. 135040–135049, 2019.
[23] S. Karimi, A. Gaillard, P. Poure, and S. Saadate, "Current sensor fault-tolerant control for WECS with DFIG," *IEEE Trans. Ind. Electron.*, vol. 56, no. 11, pp. 4660–4670, Nov. 2009.
[24] Y. Hu, L. Zhang, W. Huang, and F. Bu, "A fault-tolerant induction generator system based on instantaneous torque control (ITC)," *IEEE Trans. Energy Convers.*, vol. 25, no. 2, pp. 412–421, Jun. 2010. [Online]. Available: http://ieeexplore.ieee.org/document/5437315/
[25] M. Bermudez, I. Gonzalez-Prieto, F. Barrero, H. Guzman, M. J. Duran, and X. Kestelyn, "Open-phase fault-tolerant direct torque control technique for five-phase induction motor drives," *IEEE Trans. Ind. Electron.*, vol. 64, no. 2, pp. 902–911, Feb. 2017.
[26] J. Sun, Z. Zheng, C. Li, K. Wang, and Y. Li, "Optimal fault-tolerant control of multiphase drives under open-phase/open-switch faults based on DC current injection," *IEEE Trans. Power Electron.*, vol. 37, no. 5, pp. 5928–5936, May 2022.
[27] M. J. Durán, J. Prieto, and F. Barrero, "Space vector PWM with reduced common-mode voltage for five-phase induction motor drives operating in overmodulation zone," *IEEE Trans. Power Electron.*, vol. 28, no. 8, pp. 4030–4040, Aug. 2013.
[28] Z. Liu, Y. Li, and Z. Zheng, "A review of drive techniques for multiphase machines," *CES Trans. Elect. Mach. Syst.*, vol. 2, no. 2, pp. 243–251, Jun. 2018.
[29] M. Morawiec, K. Blecharz, and A. Lewicki, "Sensorless rotor position estimation of doubly fed induction generator based on back-stepping technique," *IEEE Trans. Ind. Electron.*, vol. 67, no. 7, pp. 5889–5899, Jul. 2020. [Online]. Available: https://ieeexplore.ieee.org/document/8917795/
[30] P. Krause, O. Wasynczuk, S. Sudhoff, and S. Pekarek, *Analysis of Electric Machinery and Drive Systems*. Hoboken, NJ, USA: Wiley, Jun. 2013, doi: 10.1002/9781118524336.

ROLAND RYNDZIONEK (Senior Member, IEEE) received the M.Sc. degree in electrical engineering from the Gdansk University of Technology (GUT), Gdansk, Poland, in 2010, the M.Sc. degree in electrical engineering from INP ENSEEIHT, Toulouse, France, in 2012, and the Ph.D. degree in electrical engineering from GUT and INP, in 2015. From 2015 to 2017, he was a Postdoctoral Research Engineer with the SuperGrid Institute, Lyon, France. Since 2017, he has been with GUT, where he is currently an Assistant Professor. His scientific and research interests include development of piezoelectric motors for embedded applications, designing of the mechatronic structures, and power converters.

KRZYSZTOF BLECHARZ received the M.Sc. degree in electrical engineering from the Czestochowa University of Technology, Czestochowa, Poland, in 2002, and the Ph.D. degree from the Gdansk University of Technology, Gdansk, Poland, in 2008. Since 2008, he has been an Assistant Professor with the Gdansk University of Technology. He is participant of many research project as a designer or a research. His research interests include doubly-fed generator control systems, multiscalar models of electrical machines, sensorless control, and nonlinear control in electric drives.

FILIP KUTT was born in Gdansk, Poland. He received the M.Sc. and Ph.D. degrees in electrical engineering from the Gdansk University of Technology (GUT), Poland, in 2007 and 2013, respectively.

He has been as an Assistant Professor with GUT, since 2007. His scientific and research interests include a wide spectrum of mathematical modeling of electrical machines using analytical modeling and FEM-based computations.

MICHAL MICHNA (Senior Member, IEEE) was born in Gdynia, Poland. He received the M.Sc. and Ph.D. degrees in electrical engineering from the Gdansk University of Technology (GUT), Poland, in 1999 and 2005, respectively.

He has been as an Assistant Professor with GUT, since 1999. His scientific and research interests include wide spectrum of mathematical modeling and diagnosis of electrical machines using analytical modeling and FEM-based computations.

GRZEGORZ KOSTRO received the Ph.D. degree in electrical engineering, in 2007. He has been involved with the Gdańsk University of Technology, since 2007, scope of his specialization are modeling, design, and diagnostics of electrical machines. He conducts research on the development of circuit models of electric machines using the Lagrange energy method, he also deals with the issues of designing electrical machines, in particular asynchronous machines with a number of phases greater than three, and low-speed synchronous generators with permanent magnets. He is the author or coauthor of three patents and 74 articles.